

## Characterization of different decomposition stages of biowaste using FT-IR spectroscopy and pyrolysis-field ionization mass spectrometry

Ena Smidt<sup>1,\*</sup>, Kai-Uwe Eckhardt<sup>2</sup>, Peter Lechner<sup>1</sup>, Hans-Rolf Schulten<sup>2</sup> & Peter Leinweber<sup>2</sup>

<sup>1</sup>*Institute of Waste Management, University of Natural Resources and Applied Life Sciences, Muthgasse 107, 1190 Vienna, Austria;* <sup>2</sup>*Institute of Soil Science, Department of Agricultural Ecology, University of Rostock, Justus-von-Liebig-Weg 6, 18059 Rostock, Germany* (\*author for correspondence: e-mail: ena.smidt@boku.ac.at)

Accepted 26 May 2004

**Key words:** composting, infrared spectroscopy, organic matter characterization, pyrolysis-field ionization mass spectrometry

### Abstract

The decomposition stage and stabilization of organic matter in biowaste (mixture of yard waste and kitchen waste), originating from an open windrow process, were investigated using Fourier transform infrared (FT-IR) spectroscopy and pyrolysis-field ionization mass spectrometry (Py-FIMS). These investigations provided detailed information about chemical constituents and their behavior during the composting process. The chemical compounds were classified by their molecular signals in Py-FIMS. Multivariate statistical analysis revealed, that during the composting process, the group containing lipids, fatty acids and other chemical compounds with aliphatic skeletons changed the most. Corresponding with Py-FIMS findings changes were observed in absorbance bands of infrared spectra that reflect this group of organic compounds: the aliphatic methylene bands at 2925 and 2850  $\text{cm}^{-1}$ , the band of C=O vibrations of carboxylates at 1640  $\text{cm}^{-1}$ , the O—H in-plane bend of carboxylic acids, the CO<sub>2</sub> stretch of carboxylates and the CH<sub>2</sub> group of alkanes at around 1430  $\text{cm}^{-1}$ . During decomposition these bands decreased up to a steady level that indicated stabilization. The band at 1260–1240  $\text{cm}^{-1}$  that can be assigned to the C—O stretch of carboxylic acids or to the C—N stretch of amides and the band of aromatic amines at 1320  $\text{cm}^{-1}$  disappeared completely. The nitrate band at 1384  $\text{cm}^{-1}$  appeared at a later stage of the composting process. The relative increase of chemical compounds like moieties of lignin, humic acids and tannins in the composted material contributed to the aromatic C=C band at around 1640  $\text{cm}^{-1}$ .

### Introduction

The stabilization of organic waste matter is a crucial requirement before being used as compost or before landfilling. For practical use and for process control, it is necessary to be able to characterize metabolic activities and stages of organic matter conversion towards a stable product. Conventional analyses focus on singular substances or the sum of substances (e.g. total organic carbon (TOC), ignition loss) and their transfor-

mation during the composting process. This approach contributes little information about the chemical and biological behavior of this material. The composition of the organic matter in soils or waste materials is very complex due to the wide range of chemical compounds and the variety of decomposed and synthesized products. Organic matter combines with inorganic compounds to build up organic–mineral complexes. The separation of organic substances is not possible without chemical changes. New analytical methods and

established methods with new applications provide insight into the entire sample of material and its chemical properties, contributing to a better understanding of the decomposition and stabilization processes taking place. Spectroscopic techniques, including Fourier transform infrared (FT-IR) spectroscopy and pyrolysis-field ionization mass spectrometry (Py-FIMS), are among the more promising tools for characterizing the chemical transformation of organic matter.

Infrared spectroscopy is based on the interaction of infrared light with matter and sensitive to present chemical functional groups (Hesse et al. 1995; Smith 1999). Humic substances originating from composts were characterized by Chen et al. (1996), Filip et al. (2000), Ouattmane et al. (2002), Sanchez-Monedero et al. (2002) and Zach & Schwanninger (1999). FT-IR spectra revealed the transformation of organic matter during a composting process (Chen & Inbar 1993). FT-IR spectroscopy was applied for assessing compost maturity (Ouattmane et al. 2000; Smidt et al. 2002). A literature review about the application of infrared spectroscopy and pyrolysis to maturity determination of composts was given by Chen (2003).

Py-FIMS enables to separate and identify chemical compounds of a sample after thermal degradation and ionization (Leinweber & Schulten 1998). Py-FIMS has been used for the characterization of organic matter in complex biomaterials. Entire soil samples, water extracts and humic substances were investigated by means of Py-FIMS (Schnitzer & Schulten 1995; Schulten 1996; Schulten et al. 1998). A colorimetric maturity test for compost was evaluated using Py-FIMS (Schnitzer et al. 1993). Furthermore, Py-FIMS was used for characterizing four phases of cow manure composting (van Bochove et al. 1996). Veeken et al. (2001) investigated the evolution of macromolecules in a composting process of wheat straw and pig manure using pyrolysis gas chromatography-mass spectrometry.

Modern spectroscopic methods such as FT-IR spectroscopy and Py-FIMS appear to be promising for the assessment of qualitative changes in waste materials. This has already been shown for composting by Leinweber et al. (2001) and Chen (2003). Of the two methods FT-IR spectroscopy offers several advantages including the low cost and little time required for sample preparation and

measurement, which make IR spectroscopy suitable to practical use. On the other hand, despite higher costs, Py-FIMS provides detailed insight into the molecular building blocks of composts and can identify general chemical fingerprints and assess quality.

The objective of the present investigation was to combine FT-IR spectroscopy and Py-FIMS in order to discover which information these techniques can contribute towards characterizing different stages of organic matter during degradation and stabilization in an open windrow process. It was important to find out the applicability of the methods in operational processes under realistic conditions. The main interest concentrated on relevant bands of the IR spectrum and identified masses in the mass spectrum that can be considered as indicators for degradation and stabilization of organic matter during the composting process.

## Materials and methods

### *Description of materials*

A mixture of yard waste and biowaste (kitchen waste including fruits, vegetables, plant materials), obtained from various recycling bins throughout Vienna, was composted in an outdoor plant. The active-decomposition phase of 4 weeks took place in a windrow. The material was rotated daily for 7 days and then twice a week for 21 days. For the curing phase of 8 months the compost was piled after 28 days and turned once a month. In total, 47 samples representing different stages of the composting process, were collected during a period of 260 days.

At every sampling date three samples were taken within the same small section from the center of the windrow. These three samples were mixed into a composite sample and sieved through 20 mm screen according to sample preparation for required compost analyses (Binner et al. 1998). The composite samples were air-dried, ground in an agate mill and sieved again (<0.63 mm).

Chemical analyses and IR spectroscopic investigations were performed for all 47 samples. Six samples selected for Py-FIMS should represent the reactive phase of the process and the final product.

All analyses were carried out from the same representative subsample.

#### *Chemical analysis*

The ignition loss was determined by incineration at 545 °C. Total carbon (TC), total inorganic carbon (TIC) and total nitrogen contents (TN) were analyzed by combustion in a Variomax CNS analyzer. TOC was calculated by the difference between TC and TIC. All analyses were carried out twice.

Humic substances were extracted using a 0.1 mol l<sup>-1</sup> solution of sodium pyrophosphate (pH 10.5). Different fractions were separated according to their solubility in acidic or alkaline solutions (Gerzabek et al. 1993). Their optical densities were measured photometrically at 400 nm.

#### *FT-IR spectroscopic investigations*

For spectroscopic investigations the sample preparation was carried out as described for chemical analyses. Two milligrams of the prepared material were pressed with (FT-IR grade) KBr (1:100) to a pellet. The pellet was immediately measured in the spectrometer after preparation under ambient conditions using the transmission mode. The measurements were carried out in the mid-infrared range from 4000 to 400 cm<sup>-1</sup> with a Bruker Equinox 55 FTIR-spectrometer at the Institute of Chemistry (University of Natural Resources and Applied Life Sciences, Vienna). The resolution was set to 4 cm<sup>-1</sup>, 32 scans were recorded, averaged for each spectrum and corrected against ambient air as background. Ten band heights were measured to a chosen baseline and corrected by the software Perkin Elmer 'Spectrum lite' corresponding to the baseline. For the comparison of different stages of decomposition relative absorbances of distinct bands were calculated, in order to even out slight weight differences and to emphasize the relative change (Haberhauer et al. 1998).

The relative absorbance (%) is the corrected band height of one distinct band multiplied by 100 and divided by the sum of all compared corrected band heights. The course of relative absorbances reflects the dynamics of the process.

Spectra in the second derivative mode could give several detailed information about weak bands.

#### *Pyrolysis-Field ionization mass spectrometry (Py-FIMS)*

Six samples representing 1, 4, 14, 32, 66 and 260 days of the composting process were selected and investigated using a temperature-resolved Py-FIMS. About 8 mg of the air dried, ground, sieved (<0.63 mm) and homogenized sample were thermally degraded by pyrolysis in the ion source (emitter: 8 kV, other electrode -3 kV) of the double-focusing Finnigan MAT 731. The samples were heated in the vacuum from 110 to 700 °C, in temperature steps of 10 °C. Between magnetic scans the emitter was flash heated to avoid residues of pyrolysis products. About 60 spectra were recorded in the mass range from 15 to 900 Da and summed using a Maspec II data system. Two to three replicates were analyzed for each sample, depending on the agreement of the mass spectra. These replicated mass spectra were averaged. The ion intensities were referred to 1 mg of the sample. For interpretation, marker signals (*m/z*) that are assigned to relevant substance groups, were used according to Schnitzer & Schulten (1992), Schulten (1996), van Bochove et al. (1996) and Leinweber et al. (2001).

#### *Statistical analysis*

The results of Py-FIMS were analyzed by principal component analysis (PCA). The PCA reduces the dimensionality of the data set to a few principal components (PC) containing most of the total variance in original variable space. In the present study principal components (PC) were calculated from the integrated mass spectrum in the range *m/z* 55 to 500 and from the 13 *m/z* with highest discriminating power between the six classes (day 1, 4, 14, 32, 66 and 260). The 13 selected *m/z* values were those with the highest variance weight, which is a ratio of interclass variance of a variable to intraclass variance. Results of PCA analysis are visualized as plots of the first versus the second principal component.

### **Results and discussion**

#### *Characterization by conventional parameters*

Decomposition of organic matter took place very slowly. The initial ignition loss of 45.1% decreased

Table 1. Ignition loss (IL) total organic carbon (TOC), total nitrogen (TN) contents and standard deviation of six selected samples

Sample (days)	IL (% of dry matter)	TOC (% of dry matter)	TN (% of dry matter)
1	45.1 ( $\pm 0.63$ )	21.5 ( $\pm 0.45$ )	1.2 ( $\pm 0.01$ )
4	48.9 ( $\pm 0.25$ )	26.2 ( $\pm 0.20$ )	1.4 ( $\pm 0.02$ )
14	49.5 ( $\pm 0.05$ )	26.5 ( $\pm 0.15$ )	1.4 ( $\pm 0.01$ )
32	46.9 ( $\pm 0.45$ )	24.8 ( $\pm 0.05$ )	1.6 ( $\pm 0.01$ )
66	44.2 ( $\pm 0.20$ )	23.9 ( $\pm 0.10$ )	1.8 ( $\pm 0.01$ )
260	40.7 ( $\pm 0.05$ )	22.7 ( $\pm 0.05$ )	1.9 ( $\pm 0.01$ )

to a final content of 40.7%. The TN content increased from 1.2% to 1.9% of dry matter (2.6–4.7% referred to the ignition loss), due to the relative rise of nitrogen during degradation. Table 1 summarizes several data of the six selected samples that were investigated by Py-FIMS. The low value of the ignition loss in the first sample can be due to the difficulty of grounding fresh plant materials in an agate mill. Figure 1 visualizes the decrease of the ignition loss and the increase of the humic acid content during the process and reflects the dynamic of the entire process.

### Humic acids

The content of extractable humic acids increased continuously, reaching about 30% of the ignition loss after 260 days (Figure 1). This finding indicates that a shift from degradable to stable organic substances took place during the composting process. Similarly, Chen & Inbar (1993) and Hsu

& Lo (1999), found increased portions of humic acids as indicators of compost maturity.

### Characterization using FT-IR spectroscopy

FT-IR spectra of the entire sample show the changes of functional groups of compounds that characterize different stages of decomposition. Bands, representing both organic and inorganic functional groups, undergo changes during the composting process. Bands representing strictly inorganic functional groups tend to rise due to the increasing concentration of inorganic compounds as organic matter decomposes. Figure 2 shows relevant bands observed as an indication of decomposition and stabilization. IR-spectroscopic characteristics represent different stages of the composting process (4, 14 and 260 days). Table 2 summarizes the relevant bands, mentioned below and their development during the composting process. The arrows indicate their behavior with time: increase, decrease or a steady level of the bands. Most bands of organic and inorganic functional groups reached a steady level after 9–10 weeks. Several bands of organic functional groups disappeared nearly completely.

During the composting process the aliphatic methylene bands at  $2925$  and  $2850\text{ cm}^{-1}$  decreased. A small shoulder at around  $1740\text{ cm}^{-1}$  up to  $1720\text{ cm}^{-1}$ , indicating aldehydes, ketones and carboxylic acids disappeared within the first week. Because of the behavior it can be assumed that the band is primarily assigned to early decomposed or volatile compounds.

The band at  $1640\text{ cm}^{-1}$  reflects the absorption of aromatic C=C bonds and of the C=O group

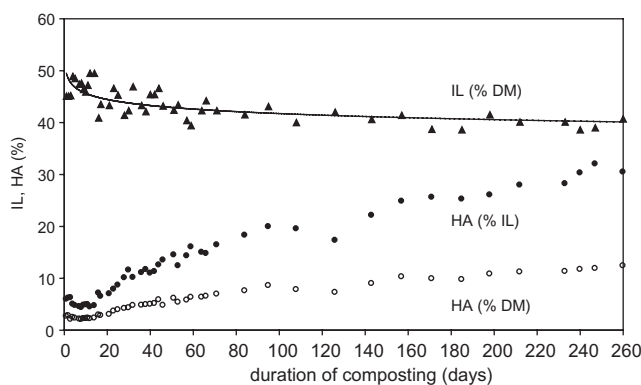


Figure 1. Ignition loss and contents of extractable humic acids during the composting process (260 days).

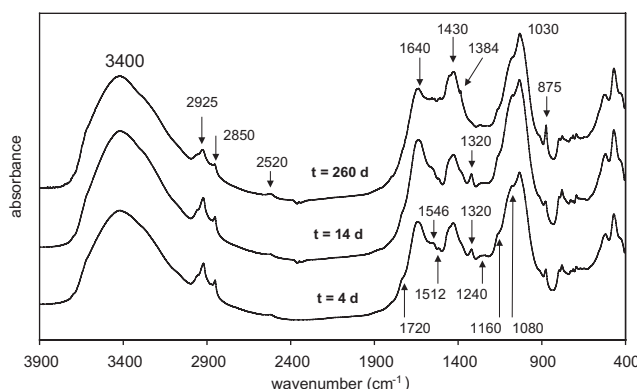


Figure 2. Relevant indicator bands and IR-spectroscopic characteristics of different decomposition stages ( $t = 4$  days,  $t = 14$  days,  $t = 260$  days).

that is part of amides or carboxylates. An ambivalent behavior was observed during the composting process. The first 2–3 weeks the band increased and after reaching a peak (4 weeks), it decreased slightly up to a nearly constant level that was higher than the starting level. This band reflects both synthesis and decomposition. Humic acids show a strong band at  $1640\text{ cm}^{-1}$  that rises during the composting process. The continuous increase of the humic acid content causes a positive impact to this band. Formation of carboxylates due to the release of carboxylic acids from decomposed lipids contributes to the rise as well.

When degradation of substances that absorb at this wavenumber exceeds synthesis, the band height decreases. The dynamics of lipids and fatty acid transformation are confirmed by Py-FIMS results. The contribution of amides to this band to the  $\text{C}=\text{O}$  vibration at  $1640\text{ cm}^{-1}$  is not clear. An increase due to the growth of microbes should be reflected by the  $\text{N}-\text{H}$  in-plane bend vibration (amide II band) in the range from  $1570$  to  $1510\text{ cm}^{-1}$  that is assigned to secondary amides. It is stronger and less overlapped by other bands than the  $\text{C}=\text{O}$  vibration. However, the band is weak in biowaste, compared to other wastes that are rich in proteins like sewage sludge (Ouatmane et al. 2000; Smidt 2001) or manure (Leinweber et al. 2001). The amide II band was found at around  $1546\text{ cm}^{-1}$ . Only the spectrum in the second derivative mode (not shown) revealed a slight increase between day 1 and 4. Then, the band decreased, reached a minimum on day 66 and increased again slightly. Py-FIMS results also indi-

cated an increase of N-containing compounds during the first 2 weeks, followed by a decrease. After 260 days higher ion intensities of masses that are attributed to peptides ( $m/z$  57, 97) were measured.

An additional effect that contributes to the rising  $1640\text{ cm}^{-1}$  band is caused by enriched chemical compounds that can be attributed to the aromatic  $\text{C}=\text{C}$  vibration, like lignin moieties and other aromatic compounds that were identified by means of Py-FIMS. It is not possible to find out the contribution of individual components to the behavior of the  $1640\text{ cm}^{-1}$  band. In addition the influence of residual water (weak absorbance band of water at  $1635\text{ cm}^{-1}$ ) has to be considered.

The band at  $1512\text{ cm}^{-1}$  (Figure 2) can be attributed to lignocellulose (Ouatmane et al. 2000). Biowaste materials are identified by this weak, but characteristic band. Other typical bands of lignin, like the vibration of the aromatic skeleton at around  $1600\text{ cm}^{-1}$  (Faix 1991) are covered by the prominent  $1640\text{ cm}^{-1}$  band.

A broad band was found at around  $1430\text{ cm}^{-1}$  due to the  $\text{O}-\text{H}$  in-plane bend of carboxylic acids, the  $\text{CO}_2$  stretch of carboxylates and the aliphatic  $\text{CH}_2$  group of alkanes (Hesse et al. 1995; Smith 1999). The  $\text{C}-\text{O}$  stretch vibration of carbonates also contributed to this band. The shape of the organic band differs from the carbonate band in that it is broader due to interactions (e.g. H-bonding). The influence of the high carbonate content of the samples (9.1–12.2% of dry matter) is clearly visible. This finding was also confirmed by another carbonate band at  $2520\text{ cm}^{-1}$  (Tseng et al.

Table 2. Summary of relevant infrared absorption bands and their development with time during the composting process (↑ = increase, ↓ = decrease, → = steady)

Wavenumber (cm <sup>-1</sup> )	Vibration	Compound or functional group	References	Development (weeks)	
				<10	>10
2925	C-H stretch	Methylene	Smith (1999)	↓	→
2850	C-H stretch	Methylene	Smith (1999)	↓	→
2520		Carbonate	Tseng et al. (1996)	↑	→
1740-1720	C=O	Aldehyde, ketone, carboxylic acids	Ouatmane et al. (2000)	↓	
			Smith (1999) Tan (1993)		
1640	C=O	Amide I, carboxylates	Haberhauer et al. (1998)	↓	→
	C≡C	Aromatic compounds	Ouatmane et al. (2000)	↑	→
			Smith (1999)		
1546	N-H in plane	Amides II	Chen et al. (1996)		
			Ouatmane et al. (2000)	↓	→
			Grube et al. (1999)		
1512		Lignocellulose	Smith (1999)		
1430	CO <sub>2</sub> stretch	Carboxylic acids	Ouatmane et al. (2000)	↓	→
	C-O stretch	Carbonate	Smith (1999)	↑	→
1384	N-O stretch	Nitrate	Hesse et al. (1995)		↑↓
			Smidt et al. (2002)		
			Zaccheo et al. (2002)		
1320	C-N stretch	Aromatic prim. and sec. amines	Smith (1999)	↑↓	
1260-1240	C-O	Carboxylic acids	Smith (1999)	↓	
	C-N	Amides	Smith (1999)		
1160	C-O-C	Polysaccharides	Grube et al. (1999)	↓	→
1080	C-O-C	Polysaccharides	Grube et al. (1999)	↓	→
1030	Si-O stretch	Clay minerals	Madejova (2003)	↑	→
	Si-O-Si	Silica	Smith (1999)		
875	C-O out of plane	Carbonate	Bosch Reig et al. (2002)	↑	→

1996). Because the organic compounds decreased during decomposition, the relative increase of inorganic components caused a rise of this band again. In the last sample the weak nitrate band at  $1384\text{ cm}^{-1}$  (Smidt et al. 2002; Zaccheo et al. 2002) is visible. The  $1320\text{ cm}^{-1}$  band can be attributed to aromatic primary and secondary amines (Smith 1999). This band showed a typical behavior of an increase followed by a decrease. After 10 weeks it had disappeared. As long as this band was present the respiration activity exceeded the limit value of  $10\text{ mg O}_2\text{ g}^{-1}\text{ 96 h}^{-1}$  dry matter (Binner et al. 1998). The pattern of this band is a reliable indicator for compost maturity (Smidt 2001). The band at around  $1240\text{ cm}^{-1}$  that can be assigned to the C—O stretch of carboxylic acids and to the C—N stretch of amides (amide III) decreased and disappeared as well during the composting process.

Polysaccharides absorb between  $1170$  and  $950\text{ cm}^{-1}$  (Tan 1993). The weak bands (shoulders) at  $1160$  and  $1080\text{ cm}^{-1}$  can be attributed to polysaccharides as reported by Grube et al. (1999), who found absorption bands of glycogen at these wavenumbers. The absorption of polysaccharides at these wavenumbers was confirmed by addition of starch or polysaccharides containing components (miscanthus, straw) to the waste material (Smidt 2001). A slight decrease of the  $1160\text{ cm}^{-1}$  band was measured during the first 9 weeks.

Silica (clay minerals) is characterized by a huge, typically shaped band at  $1030\text{ cm}^{-1}$ , due to the Si—O—Si asymmetric stretch vibration (Madejova 2003; Smith 1999). The absorption of silica at this wavenumber was confirmed by the spectrum of the ignition residue (Smidt 2001). A sharp band at  $875\text{ cm}^{-1}$  is assigned to the C—O out-of plane bend of carbonates (Bosch Reig et al. 2002; Smith

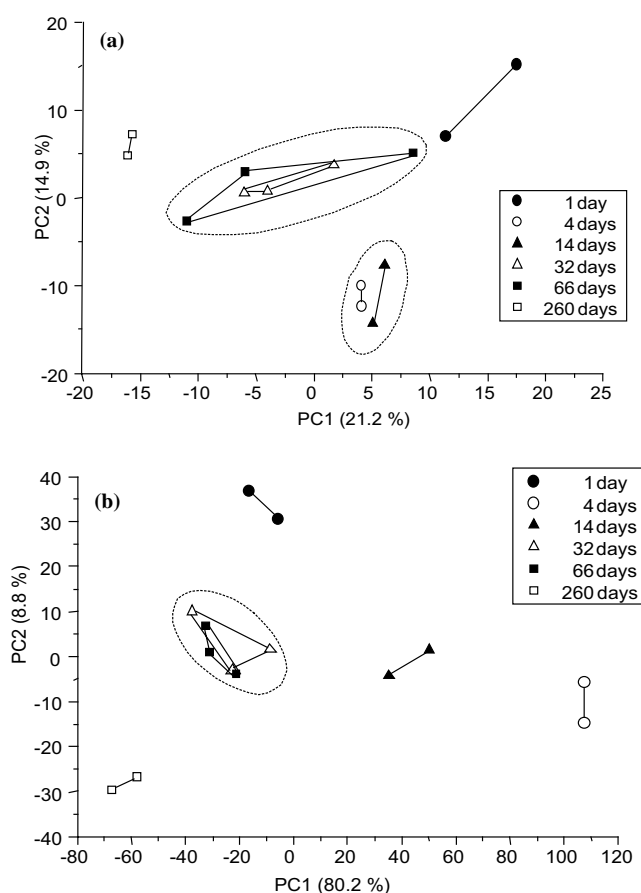


Figure 3. Principal component analysis of Py-FI mass spectra of samples from consecutive stages of biowaste composting, using all  $m/z$  from 55 to 500 (a), and the 13  $m/z$  (b) with the highest discriminating power.

1999). The bands both increase during decomposition of organic matter.

#### *Additional information using Py-FIMS*

Py-FIMS offered a more detailed insight into the molecular chemical constituents of compost. The mass spectra of the entire samples were very complex (not shown). Thus in the first step, a PCA was carried out with the signals  $m/z$  55–500 (Figure 3a). The first two PC reflected about 36.1% of variance between the samples and separated four groups of samples: (1) day 1, (2) days 4 and 14, (3) days 32 and 66, (4) day 260. Signals of  $n$ -C<sub>16</sub> ( $m/z$  256) and  $n$ -C<sub>18</sub> ( $m/z$  284) fatty acids were among the signals with the highest variance weight. In the second step (Figure 3b), the PCA using  $n = 13$   $m/z$  with the highest discriminating power also enabled to separate samples from days 4 and 14. As a result, about 65.4% of the total variance was explained by the first two components. This analysis unequivocally shows that the mass spectra were able to identify changes in the chemical composition during composting. For a better overview, only the masses that could be attributed to chemical compounds were selected for analysis and discussion. Figure 4a–d show a plot of the selected masses versus ion intensities/mg for four samples (day 1, day 4, day 14 and day 260 of the composting process). The most prominent mass signals  $m/z$  were designated, including the group of lipids, fatty acids and aliphatic compounds, sterols, N-containing compounds and peptides, carbohydrates, phenols and lignin monomers, alkylaromatics and suberin. Changes in ion intensities of different groups indicated the progress of the composting process. Table 3 summarizes the selected masses and the related compounds.

Day 4 and day 14 of composting were characterized by increasing intensities of all selected masses as reported by van Bochove et al. (1996) for cow manure compost. Most biological activity and transformation took place at this time. Biological activity was confirmed by other parameters like respiration activity, the rise and the decrease of C2–C5-carboxylic acids and the high pile temperature (Smidt 2001). The group containing lipids, fatty acids and different aliphatic compounds changed the most during the composting process. The remarkable contribution of  $n$ -C<sub>16</sub> and  $n$ -C<sub>18</sub>

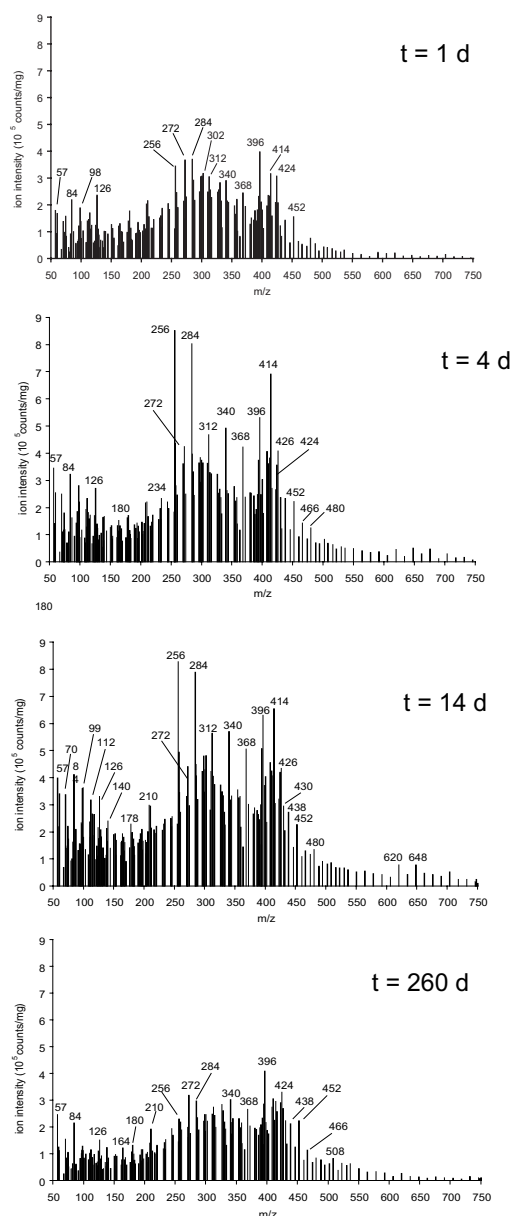


Figure 4. Changing ion intensities of selected masses ( $m/z$ ) that are attributed to chemical substance groups ( $t = 1$  days,  $t = 4$  days,  $t = 14$  days,  $t = 260$  days).

fatty acids to increasing ion intensities during the first 2 weeks can be attributed to lipid degradation and release of fatty acids and to the development of microbial biomass. In soils these chain lengths are assigned to primary organic matter and microorganisms (Jandl et al. 2002). Some of the signals that are assigned to sterols ( $m/z$  388, 390) also were among signals with largest variance



Table 3. Summary of the selected mass signals ( $m/z$ ) and related chemical compounds

Substance group	$m/z$
Lipids, fatty acids, aliphatic compounds	202, 216, 230, 244, 256, 258, 270, 272, 284, 286, 298, 300, 312, 314, 326, 328, 340, 342, 354, 368, 380, 382, 394, 396, 408, 410, 422, 424, 438, 452, 466, 480, 494, 508, 522, 536, 550, 564, 578, 592, 606, 620, 634, 648, 662, 676, 704, 718, 732, 746
Sterols	372, 386, 388, 390, 392, 394, 396, 398, 400, 402, 408, 410, 412, 414, 416, 426, 430
Peptides	57, 70, 73, 74, 75, 84, 87, 91, 97, 99, 115, 120, 129, 135
N-containing compounds	59, 67, 79, 81, 95, 103, 109, 111, 123, 125, 137, 139, 153, 161, 167, 181, 183, 195, 203, 233, 245, 255, 257, 271, 285, 333, 359, 363, 393
Phenols, lignin monomers	94, 108, 110, 122, 124, 138, 140, 150, 152, 154, 164, 166, 168, 178, 180, 182, 194, 196, 208, 210, 212
Alkylaromatics	170, 176, 184, 190, 192, 198, 204, 206, 218, 220, 232, 234, 246, 260, 274, 288, 302, 316, 330, 344, 358, 372, 386
Carbohydrates	60, 72, 82, 84, 96, 98, 110, 112, 114, 126, 132, 144, 162
Suberin	432, 446, 460, 474, 488, 502, 516, 530

weights in principal component analyses. Day 4 and 14 showed the highest ion intensity, while day 32 and 66 (not shown) were characterized by diminishing ion intensities. It is noteworthy, that some substances were relatively enriched at the end of composting: nitrogen-containing compounds ( $m/z$ : 123, 181, 255, 271, 299) and peptides ( $m/z$ : 57, 97) in the low  $m/z$  area, some chemical compounds that are assigned to the group of lipids, fatty acids, aliphatic compounds ( $m/z$ : 380, 422), sterols ( $m/z$ : 390, 408, 414, 416, 430) and suberin ( $m/z$ : 432, 446, 460, 474, 488, 502, 516, 530) in the high  $m/z$  area. Enrichment of sterols was also

found by van Bochove et al. (1996) in manure compost. Thermally stable sterols originating from plant materials were still detectable in extracted soil organic matter. The signals at  $m/z$  414 and 430 were attributed to sitosterol and  $\alpha$ -tocopherol (Schnitzer et al. 1991).

After subtraction of ion intensities (day 1 spectrum minus day 260 spectrum) the pattern of the difference spectrum (Figure 5) revealed a shift of masses due to the relative enrichment of chemical compounds with higher molecular weights and greater resistance to degradation. In addition the synthesis of larger molecules (micro-

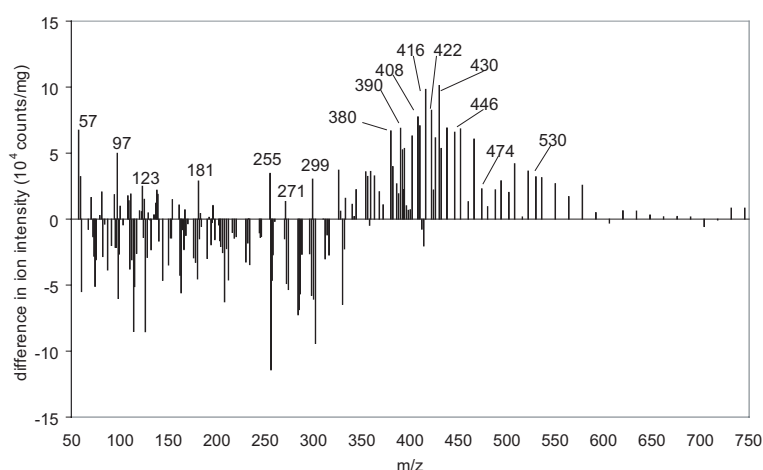


Figure 5. Subtraction of the mass spectra (day 260–day 1) revealed the general shift from lower to higher  $m/z$  (sterols: 390, 408, 414, 416, 430); compounds of the lipids/fatty acid/aliphatics group: 380, 422; suberin: 432, 446, 460, 474, 488, 502, 516, 530; refractory or synthesized nitrogen containing compounds and peptides: 57, 97, 123, 181, 255, 271, 299).

bial biomass, humic substances, biopolymers produced by microorganisms) can be responsible for the shift.

Lignin, an important compound in yard waste, is characterized by several marker signals in Py-FIMS. However, for several reasons lignin is not a suitable indicator for the progressing process. A major part of lignin-containing constituents are not included in the samples to be analyzed due to the exclusion of large particle sizes (>20 mm). Furthermore lignin is quite resistant to degradation within the time frame of composting, and to grinding in the agate mill.

The relative ion current of marker groups and ion intensities/mg showed a divergent development at the beginning, as far as carbohydrates were concerned (Figure 6). After 8–10 weeks, when stabilization was indicated by other parameters, like the low respiration activity ( $<10 \text{ mg O}_2 \text{ g}^{-1} \text{ 96 h}^{-1}$  dry matter), a stable C/N ratio of around 12, pH of 7.5, increasing humic acid content, decreasing pile temperatures and plant compatibility (Smidt 2001), the patterns of relative and absolute intensities became parallel. This finding confirmed that easily degradable substances were no longer decomposing and that the material became stabilized.

The stabilization was reflected by changes in the thermal volatilization of compounds during Py-FIMS. Therefore, the summed relative ion intensities (% TII) of molecule groups versus the temperature (110–700 °C) were plotted for samples from successive composting stages. These

plots visually illustrate changes in the thermal behavior and abundance of substance groups during the composting process. Thermograms of two substance groups (lipids/fatty acids/aliphatics group and the group of carbohydrates) are presented in Figure 7a and b. Maximal differences of peak intensities are shown: days 1 and 260 for carbohydrates, days 14 and 260 for the lipids/fatty acids/aliphatics group. Regarding the lipids/fatty acids/aliphatics group (Figure 7a), two peaks of the relative ion intensity were found in the well composted material (260 days). The maximum occurred at 350 °C and a second peak at 500 °C. The 14-day old material had two peaks below 300 °C and the maximum at 350 °C. The group of lipids/fatty acids/aliphatics includes a wide range of different chemical compounds. Volatile, low molecular compounds are characterized by peaks at lower temperatures. Such compounds disappear during the composting process and non-volatile, high molecular weight compounds are relatively enriched. Due to their resistance to thermal degradation they cause a peak shift towards higher temperatures. In addition interactions with inorganic compounds give rise to the same effect. In contrast Figure 8b shows the uniform thermal behavior of carbohydrates that were identified as marker. All samples had a maximum of relative ion intensities at the same temperature (350 °C). Due to degradation by microorganisms the contribution of carbohydrates to the total ion current decreased. But carbohydrates are not metabolized completely. Cellulose is still found in the degraded

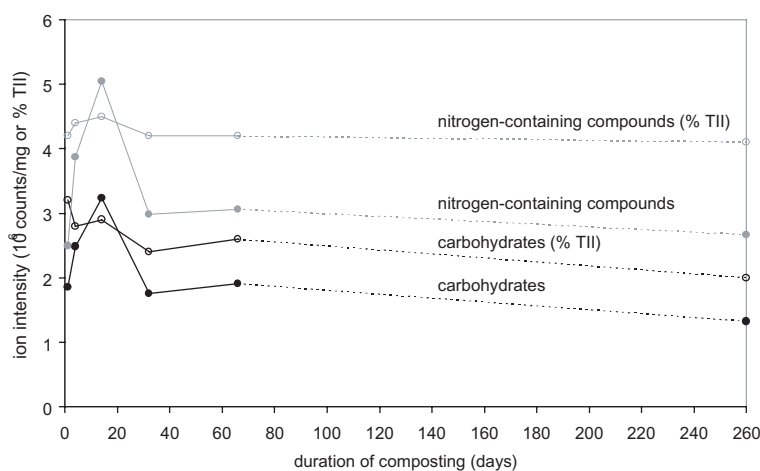


Figure 6. The development of relative and absolute ion intensities of nitrogen-containing compounds and carbohydrates (TII = total ion intensity).

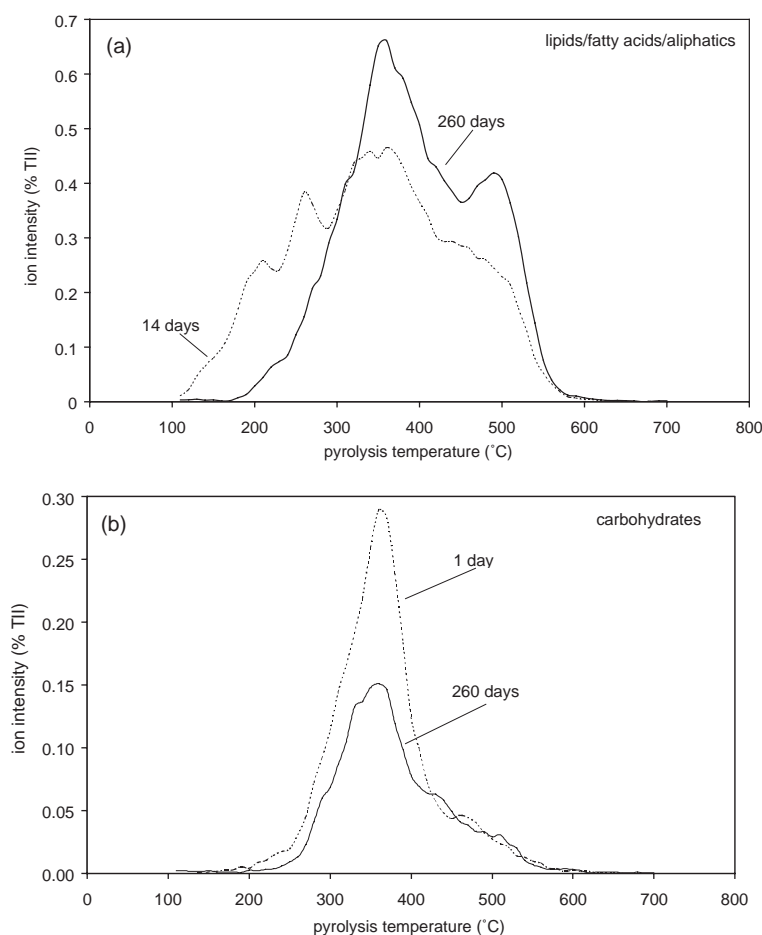


Figure 7. Thermograms (a) of the lipids/fatty acids/aliphatics group (day 14 and day 260 of composting) and thermograms (b) of the carbohydrates group (day 1 and day 260 of composting); TII = total ion intensity.

and stabilized organic matter fraction of composts. Mineral compounds have a protecting effect on biomolecules. In addition microbial carbohydrates (starch like molecules, glycogen) are synthesized. The weak band at  $1160\text{ cm}^{-1}$  corresponds to Py-FIMS results.

This evaluation confirms general evidence of changes in the thermal behavior during composting due to enrichment of non-volatile, high molecular weight compounds, synthesis of microbial biomass and chemical transformation (e.g. humic substance formation). The contribution of physical stabilization processes, like incorporation of organic molecules into inorganic aggregates or fixation on clay minerals has to be taken into consideration as well (Baldock & Skjemstad 2000; Wershaw et al. 1996). This evidence was previously demonstrated by other thermal methods, like

thermogravimetry and differential scanning calorimetry (Blanco & Almendros 1994; Dell'Abate et al. 1997; Oades 1993; Otero et al. 2002; Ouattmane et al. 2000). In the present investigation, these general thermal changes could be assigned to individual substance groups.

## Conclusions

Py-FIMS as well as FT-IR spectroscopy confirmed that stabilization took place after 8–10 weeks of composting. These results agree with chemical and biological evidence as described in the Py-FIMS section.

Representative samples are a prerequisite to assess a composting process. This requirement has to be solved by means of a good sampling design.

The fraction <20 mm represents the relevant particle sizes of metabolic activities and reflects the development of organic matter. FT-IR spectroscopy and Py-FIMS are carried out with very small sample amounts of a few milligrams. With the described sample preparation a very good reproducibility was available. For the comparison of the spectroscopic methods with conventional parameters all investigations should be carried out from the same representative subsample.

Py-FIMS is primarily applied in the scientific field. In contrast, the application of FT-IR spectroscopy in composting plants seems very promising due to the advantages mentioned in the introduction. The relevant absorbance bands of biowaste spectra show a characteristic behavior during the composting process as indicated by the arrows in Table 2. Stabilization is proved by the absence of several bands (1740–1720, 1320, 1260–1240  $\text{cm}^{-1}$ ) and the steady level of organic and inorganic band heights. The appearing nitrate band at 1384  $\text{cm}^{-1}$  indicates a later stage of composting. These characteristic features of compost spectra provide the qualitative assessment of organic matter stability and compost maturity.

Band intensities and time scale depend on the mixture of biowaste materials and the applied technology (Smidt 2001; Smidt et al. 2002). Therefore it is not useful to indicate definite values of band heights. They should be determined under specific conditions of the composting plant. Then, process control and quality assessment of the final product are carried out by comparison of spectroscopic characteristics.

## Acknowledgements

We would like to thank Dr. B. Hinterstoisser and Dipl. Ing. M. Schwanninger, who placed the FT-IR Spectrometer of the working group “Wood Chemistry” (University of Natural Resources and Applied Life Sciences, Vienna) at our disposal and Dr. R. Beese (University of Rostock) who carried out the Py-FIMS investigations.

## References

- Baldock JA & Skjemstad JO (2000) Role of soil matrix and minerals in protecting natural organic materials against biological attack. *Org. Geochem.* 31: 697–710
- Binner E, Zach A, Widerin M & Lechner P (1998) Auswahl und Anwendbarkeit von Parametern zur Charakterisierung der Endprodukte aus mechanisch-biologischen Restmüllbehandlungsverfahren, Teil 3. Schriftenreihe des Bundesministeriums für Umwelt, Jugend und Familie, Wien
- Blanco MJ & Almendros G (1994) Maturity assessment of wheat straw composts by thermogravimetric analysis. *J. Agric. Food Chem.* 42: 2454–2459
- Bochove van E, Couillard D, Schnitzer M & Schulten H-R (1996) Pyrolysis-field ionization mass spectrometry of the four phases of cow manure composting. *Soil Sci. Soc. Am. J.* 60: 1781–1786
- Bosch Reig F, Gimeno Adelantado JV & Moya Moreno MCM (2002) FTIR quantitative analysis of calcium carbonate (calcite) and silica (quartz) mixtures using the constant ratio method. Application to geological samples. *Talanta* 58: 811–821
- Chen Y (2003) Nuclear magnetic resonance, infrared and pyrolysis: application of spectroscopic methodologies to maturity determination of composts. *Compost Sci. Util.* 11/2: 152–168
- Chen Y & Inbar Y (1993) Chemical and spectroscopical analyses of organic matter transformations during composting in relation to compost maturity. In: Hoitink HAJ & Keener HM (Eds) *Science and Engineering of Composting: Design, Environmental, Microbiological and Utilization Aspects* (pp 551–600). The Ohio State University
- Chen Y, Chefetz B & Yitzhak H (1996) Formation and properties of humic substance originating from composts. In: de Bertoldi M, Sequi P, Lemmes B & Papi T (Eds) *The Science of Composting Part 1* (pp 382–393). Blackie Academic and Professional, Chapman and Hall, London
- Dell’Abate MT, Canali S, Trinchera A, Benedetti A & Sequi P (1997) Evaluation of the stability of organic matter in composts by means of humification parameters and thermal analysis. In: Drozd J et al. (Eds) *The Role of Humic Substances in the Ecosystems and Environmental Protection* (pp 842–846)
- Faix O (1991) Classification of lignins from different botanical origins by FTIR-spectroscopy. *Holzforschung* 45: 21–27
- Filip Z, Pecher W & Berthelin J (2000) Microbial utilization and transformation of humic acid-like substances extracted from a mixture of municipal refuse and sewage sludge disposed of in a landfill. *Environ. Pollut.* 109: 83–89
- Gerzabek MH, Danneberg O & Kandeler E (1993) Bestimmung des Humifizierungsgrades. In: Schinner F, Öhlinger R, Kandeler E & Margesin R (Eds) *Bodenbiologische Arbeitsmethoden* (pp 107–109). Springer Verlag
- Grube M, Zagreba E, Gromozova E & Fomina M (1999) Comparative investigation of the macromolecular composition of mycelia forms *Thielavia terrestris* by infrared spectroscopy. *Vibr. Spectrosc.* 19: 301–306
- Haberhauer G, Rafferty B, Strebl F & Gerzabek MH (1998) Comparison of the composition of forest soil litter derived from three different sites at various decomposition stages using FT-IR spectroscopy. *Geoderma* 83: 331–342
- Hesse M, Meier H & Zeeh B (1995) *Spektroskopische Methoden in der organischen Chemie*. Georg Thieme Verlag, Stuttgart
- Hsu J-H & Lo S-L (1999) Chemical and spectroscopic analysis of organic matter transformations during composting of pig manure. *Environ. Pollut.* 104: 189–196

- Jandl G, Schulten H-R & Leinweber P (2002) Quantification of long-chain fatty acids in dissolved organic matter and soils. *J. Plant. Nutr. Soil Sci.* 165: 133–139
- Leinweber P & Schulten H-R (1998) Advances in analytical pyrolysis of soil organic matter. *J. Anal. Appl. Pyrolysis* 47: 165–189
- Leinweber P, Wehner A & Schulten H-R (2001) Qualitätsbeurteilung von Komposten aus Bioabfällen mit klassischen biologischen und chemischen sowie mit modernen spektroskopischen Methoden (pp 493–515). *ATV-Handbuch*, Verlag Ernst, Berlin
- Madejova J (2003) FTIR techniques in clay mineral studies. *Vibr. Spectrosc.* 31: 1–10
- Oades JM (1993) The role biology in the formation, stabilization and degradation of soil structure. *Geoderma* 56: 377–400
- Otero M, Calvo LF, Estrada B, Garcia AI & Moran A (2002) Thermogravimetry as a technique for establishing the stabilization progress of sludge from wastewater treatment plants. *Thermochim. Acta* 389: 121–132
- Ouatmane A, D'Orazio V, Hafidi M & Senesi N (2002) Chemical and physicochemical characterization of humic acid-like materials from composts. *Compost Sci. Util.* 10/1: 39–46
- Ouatmane A, Provengano MR, Hafidi M & Senesi N (2000) Compost maturity assessment using calorimetry, spectroscopy and chemical analysis. *Compost Sci. Util.* 8: 124–134
- Sanchez-Monedero MA, Cegarra J, Garcia D & Roig A (2002) Chemical and structural evolution of humic acids during organic waste composting. *Biodegradation* 13: 361–371
- Schnitzer M & Schulten H-M (1992) The analysis of soil organic matter by pyrolysis-field ionization mass spectrometry. *Soil Sci. Soc. Am. J.* 56: 1811
- Schnitzer M & Schulten H-R (1995) Analysis of organic matter in soil extracts and whole soils by pyrolysis-mass spectrometry. *Adv. Agron.* 55: 167–217
- Schnitzer M, Dincl H, Mathur SP, Schulten HR & Owen G (1993) Determination of compost biomaturity. III. Evaluation of a colorimetric test by <sup>13</sup>C-NMR spectroscopy and pyrolysis-field ionization mass spectrometry. *Biol. Agric. Hortic.* 10: 109–123
- Schnitzer M, Schulten HR, Schuppli P & Angers DA (1991) Organic matter extraction from soils with water at high pressures and temperatures. *Soil Sci. Soc. Am. J.* 55: 102–108
- Schulten H-R (1996) Direct pyrolysis-mass spectrometry of soils: A novel tool in agriculture, ecology, forestry and soil science. In: Yamasaki S & Boutton TW (Eds) *Mass Spectrometry of Soils* (pp 373–436). Dekker, New York
- Schulten H-R, Leinweber P & Schnitzer M (1998) Analytical pyrolysis and computer modelling of humic and soil particles. In: Huang PM, Senesi N & Buffle J (Eds) *Environmental Particles: Structure and Surface Reactions of Soil Particles* (pp 281–324). Wiley, Chichester
- Smidt E (2001) Eignung der FT-IR Spektroskopie zur Charakterisierung der organischen Substanz in Abfällen. Phd thesis, University of Agricultural Sciences, Inst. of Waste Management, Vienna, Austria
- Smidt E, Lechner P, Schwanninger M, Haberhauer G & Gerzabek MH (2002) Characterization of waste organic matter by FT-IR spectroscopy – application in waste science. *Appl. Spectrosc.* 56: 1170–1175
- Smith B (1999) *Infrared Spectral Interpretation*. CRC Press, Boca Raton, London, New York, Washington, DC
- Tan KH (1993) Humus and humic acids. In: *Principles of Soil Chemistry: Colloidal Chemistry of Organic Soil Constituents* (pp 79–127). M. Dekker Inc
- Tseng DY, Vir R, Traina SJ & Chalmers JJ (1996) A Fourier-Transform Infrared Spectroscopic Analysis of Organic Matter Degradation in a Bench-Scale Solid Substrate Fermentation (Composting) System. *Biotechnol. Bioeng.* 52: 661–671
- Veeken AHM, Adani F, Nierop KGJ, de Jager PA & Hamelers HVM (2001) Degradation of biomacromolecules during high-rate composting of wheat straw – amended feces. *J. Environ. Qual.* 30: 1675–1684
- Wershaw RL, Llaguno EC, Leenheer JA, Sperline RP & Song Y (1996) Mechanism of formation of humus coatings on mineral surfaces 2. Attenuated total reflectance spectra of hydrophobic and hydrophilic fractions of organic acids from compost leachate on alumina. *Colloids Surf. A: Physicochem. Eng. Aspects* 108: 199–211
- Zaccheo P, Ricca G & Crippa L (2002) Organic matter characterization of composts from different feedstocks. *Compost Sci. Util.* 10/1: 29–38
- Zach A & Schwanninger M (1999) Charakterisierung von Huminsäuren aus Abfallstoffen mittels FT-IR. *Österreichische Wasser- und Abfallwirtschaft* 11: 333–340